PHOTOSYNTHETICA
International Journal for Photosynthesis Research

DOI 10.32615/ps.2026.012 PHOTOSYNTHETICA 64 (2): 95-109, 2026

Drought stress-induced changes in PSII functioning in ecologically contrasting plants: chlorophyll fluorescence study of poikilohydric and homoiohydric species

J. HÁJEK[*], A. PUHOVKIN[**,***,#,##], J. LANG[###], S.I. UL HAQ[**], M. BERNATOVÁ[*], D. GIORDANO[**], J. SEKERÁK JR.[**], and M. BARTÁK[**,+]

Department of Forest Protection and Wildlife Management, Faculty of Forestry and Wood Technology, Mendel University, Zemědělská 3, 613 00 Brno, Czech Republic[*]
Department of Experimental Biology, Laboratory of Photosynthetic Processes, Faculty of Science, Masaryk University, Kamenice 5, C-13, 625 00 Brno, Czech Republic[**]
Institute for Problems of Cryobiology and Cryomedicine, National Academy of Science of Ukraine, Pereyaslavska Str. 23, 61016 Kharkiv, Ukraine[***]
National Antarctic Scientific Centre, State Institution, Ministry of Education and Science of Ukraine, Taras Shevchenko Blvd. 16, 01601 Kyiv, Ukraine[#]
Department of Geography, Faculty of Science, Masaryk University, Kotlářská 2, 611 37 Brno, Czech Republic[##]
Agricultural Research, Ltd., Zahradní 1, 664 41 Troubsko, Czech Republic[###]

Abstract

Dehydration reduces photosynthetic performance in leaves and other photosynthetic organs in response to drought. This decline is linked to changes in chlorophyll fluorescence, which reflects reduced photosystem II activity and increased protective non-photochemical quenching (NPQ). This study examined NPQ dynamics during desiccation across diverse species, including lichens, mosses, conifers, crops, and C_3 and C_4 plants, using the method of NPQ induction and relaxation curves. Gradual dehydration from a full-hydration state (RWC 100%) to complete dryness (RWC 0%) was applied in order to compare poikilohydric and homoiohydric species. NPQ_{max} (light period), NPQ_{relax} (dark period end), and the initial slopes of NPQ rise (α) and decline (β) were evaluated. Relative electron transport rate curves were also assessed. Results showed the above NPQ parameters are highly sensitive to dehydration, suggesting their usefulness – along with standard maximum (F_V/F_M) and effective quantum yield (Φ_{PSII}) – as early indicators of drought stress in PSII across plant groups.

Keywords: desiccation; F_V/F_M; non-photochemical quenching; relative water content.

Highlights

- Non-photochemical quenching induction/relaxation curves indicate drought stress
- Critical water content for PSII activity is lower in poikilo- than homoiohydric plants
- During desiccation, the share of energy to photoinhibitory quenching is species-specific

Received 27 October 2025
Accepted 19 May 2026
Published online 10 June 2026

[+]Corresponding author
e-mail: mbartak@sci.muni.cz

Abbreviations: ChlF – chlorophyll fluorescence; DM – dry mass; F_o – minimum ChlF; F_o' – dark-adapted background ChlF; F_M – maximum ChlF; FM – fresh mass; F_M' – maximum ChlF reached after an SP is applied in the light-adapted state (at the end of the light period); F_M'' – maximum ChlF after the application of the SP at the end of the dark period (180 seconds after the actinic light was switched off; FMDD – fresh mass during desiccation; F_t – ChlF recorded at the end of the light period; F_V/F_M – maximum quantum yield of photochemical processes in PSII for light-acclimated state; F_V'/F_M' – maximum quantum yield of PSII in the light-adapted state; NPQ – non-photochemical quenching; q_E – energy-dependent quenching; q_I – photoinhibitory quenching; q_{I+T} – photoinhibitory and state transition-related quenching; q_P – photochemical quenching; rETR – relative electron transport rate; RWC – relative water content; RWC_{50} – the RWC value at which F_V/F_M reaches half of its maximum value; RWC_{crit} – the RWC value at which F_V/F_M was fully limited and reached zero; RWC_{init} – the RWC range at which F_V/F_M values do not show any substantial decrease during the initial phase of desiccation; α parameter – the slope of the initial part of NPQ induction; β parameter – the slope of the initial NPQ decrease at the beginning of the dark period (relaxation curve); $\Phi_{f,D}$ – quantum yield of constitutive nonregulated energy dissipation; Φ_{NPQ} – quantum yield of non-photochemical quenching; Φ_{PSII} – effective quantum yield of PSII chemistry for light-acclimated state.

Acknowledgements: The authors acknowledge the support from the VAN (Ministry of Education, Youth, and Sports of the Czech Republic) CARP MU project (2024-2026) that provided some instruments and laboratory infrastructure for measurements.
Conflict of interest: The authors declare that they have no conflict of interest.

Introduction

Over the last few decades, global warming has increased air temperatures in most terrestrial ecosystems on Earth. The latest climate change scenario suggests that air temperatures will rise by 1.5–2.0°C by 2100. Such changes will have numerous consequences for terrestrial habitats – for example, an increased frequency of heatwaves, precipitation deficits and risks associated with low water availability and consequent droughts (Hoegh-Guldberg *et al.* 2018). It is well established that high temperatures and drought stress cause numerous negative changes in plant physiological processes (Seleiman *et al.* 2021), including direct thermal effects on the composition and structure of plants, which result in changes in membrane fluidity and a consequent limitation of biochemical processes.

Drought stress, caused by limited soil water availability, reduces stomatal conductance, limiting water loss from leaves. Stomatal responses to combined drought and high temperatures vary among species (Marchin *et al.* 2022), but generally reduce photosynthesis and transpiration, as the two processes are closely linked under a wide range of environmental conditions. Under severe drought stress, nonstomatal limitation of photosynthesis occurs, which is associated with diffusive resistance at the leaf level – that is, mesophyll and chloroplast conductance of CO_2 (Flexas and Medrano 2002). Nonstomatal limitation is accompanied by metabolic impairment, such as biochemical limitation of photosynthesis. Because stomatal and nonstomatal limitations act simultaneously, the net photosynthetic CO_2 fixation declines (Lu *et al.* 2015), along with plant growth and development (Granda and Camarero 2017). Negative effects on PSII are further intensified when drought is combined with additional stressors, such as high photosynthetically active radiation (PAR) (Hazrati *et al.* 2016) and heat (Barboričová *et al.* 2022).

Apart from the biochemical processes of photosynthesis, the biophysical processes related to PAR absorption, its utilisation in chloroplasts and the production of ATP and NADP are also limited under drought stress. Numerous studies have reported a drought-induced decrease in chlorophyll fluorescence parameters (ChlF) related to the PSII supercomplex function. Among these are a decrease in two protein complexes associated with the PSII light-harvesting complexes (LHCs) – for example, Lhcb2 and Lhcb1 – along with the OEC-related protein complexes (Dalal and Tripathy 2018). A decline in the maximum quantum yield of photochemical processes in PSII for the light-acclimated state (F_V/F_M) has also been reported (Wang *et al.* 2022). However, this parameter is sometimes considered unreliable, as some plant species exhibit sensitivity in their F_V/F_M response to drought stress, while others do not (reviewed by Banks 2018).

Drought-induced reductions in ChlF related to photosynthetic electron transport – such as the effective quantum yield of PSII chemistry for light-acclimated state (Φ_{PSII}) and relative electron transport rate (rETR) – have been reported to decline under drought stress across a wide range of plants, including C_3 crops (Zlatev 2009), C_4 crops (Xu *et al.* 2008), broadleaf trees (Kitao *et al.* 2021), and coniferous trees (Swoczyna *et al.* 2022).

Fast ChlF transient response (OJIP) and its derived parameters represent another approach that provides insight into PSII function under drought stress. Recent studies using the OJIP method have addressed various aspects of altered energy fluxes and their effectiveness in the PSII function of drought-treated vascular plants (Meng *et al.* 2016) and poikilohydric lichens and mosses (Puhovkin *et al.* 2022) during desiccation.

Among the methods used to evaluate drought stress effects on PSII and the primary biophysical processes of photosynthesis, non-photochemical quenching (NPQ) induction and relaxation curves play an important role, as they enable the assessment of drought-dependent involvement of protective mechanisms. Since the 1990s, NPQ induction and relaxation curves have been widely used to evaluate protective quenching mechanisms in *Arabidopsis thaliana* mutations, particularly those with modified capacities to quench excess light energy (Niyogi *et al.* 1998). These studies utilised *A. thaliana* mutations with either an enhanced or suppressed ability to induce NPQ, addressing various aspects of NPQ regulation.

Studies on *A. thaliana* mutants have examined the effects of the absence of minor antenna complexes on NPQ (Townsend *et al.* 2018), the impact of violaxanthin de-epoxidase and the absence of zeaxanthin (Acebron *et al.* 2020), and the role of PsbS proteins (Li *et al.* 2002) in determining the proportions of nonregulated and regulated energy dissipation in PSII (Ikeuchi *et al.* 2016). It is well established that significant differences in NPQ activation exist between species with different growth strategies and drought resistance. Drought-tolerant species exhibit higher NPQ capacity than drought-sensitive ones, reflected in the rapid activation and deactivation of underlying NPQ mechanisms.

The latter aspect is studied through NPQ induction and relaxation kinetics, which have been employed in comparative studies to assess species- or genotype-specific NPQ as influenced by external factors such as nitrogen availability (Sahay *et al.* 2024), short-term photoinhibition (Barták *et al.* 2023), and species-specific differences in lichens (Beckett *et al.* 2021a), especially those exhibiting different light acclimation properties, including light and shade ecotypes (Mkhize *et al.* 2022).

Since stress alters the shape of NPQ induction and relaxation curves compared to controls, the values were fitted using an exponential function to assess treatment effects. This approach enables the rapid testing of hundreds of genotypes for activity using a photosynthetic apparatus within a single day (Gotarkar *et al.* 2022), facilitating the evaluation of the protective mechanisms in chloroplasts.

The NPQ induction and relaxation method holds great potential, not only for screening mutations but also for monitoring desiccation-induced changes in photosynthetic performance in both field- and laboratory-based studies. Consequently, it applies to experimental plant physiology. This study evaluates the sensitivity of specific ChlF derived from NPQ induction and relaxation curves to different

drought levels in the assimilation tissues of ecologically contrasting species, including lichens and vascular plants with C_3 and C_4 metabolisms, as well as broadleaf and coniferous tree species.

Furthermore, we correlated the NPQ induction and relaxation kinetic parameters with those derived from the F_V/F_M and Φ_{PSII} desiccation response curves to identify the most reliable indicators of early, mid and severe drought stress effects on PSII.

Materials and methods

The evaluated species: Several contrasting species from different habitats and with different growth strategies were selected for measurements of desiccation-dependent changes in the ChlF parameter. These species included crops (*Solanum lycopersicum*, *Malva moschata* – C_3 plants, *Zea mays* – a C_4 plant), poikilohydric nonvascular plants and organisms (a moss, *Polytrichum strictum*; liverwort, *Marchantia polymorpha*; and a lichen, *Hypogymnia physodes*), and two conifers (*Pinus mugo*, *Cedrus libani*). For a detailed description of the experimental plants, *see Supplement*.

Cultivation and handling of the species under evaluation: *Z. mays* was grown hydroponically in a liquid medium. *M. moschata* was potted in a growth substrate (*RS I substrate*, *Agro Profi*, Říkov, Czech Republic – for nutrient composition, *see Supplement*). Poikilohydric organisms (*P. strictum*, *M. polymorpha*, and *H. physodes*) were collected from the field and transferred to the laboratory in a dry state (dried naturally in the field in a shady and windy location). After collection, they were rewetted for 48 h.

For the conifers, shoots bearing at least three cohorts of needles were cut off in the field, wrapped in wet paper and stored in a portable fridge with an electrically controlled temperature of 5°C. After transfer to the laboratory, they were left to acclimatise to laboratory temperature (23°C) for four hours. Typically, 20 needles from the current year were detached from the shoots and used in the measurements. Details of the cultivation of *Z. mays* and *M. moschata*, as well as a description of the collection sites of the other evaluated species, are provided in Table 3S (*Supplement*).

Desiccation of samples: For the measurement of ChlF during desiccation, round-shaped leaf/thallus segments with an area of 4 cm² were cut from the leaves/thalli. For the conifers, individual needles were cut longitudinally into two pieces to promote desiccation. For measurement, leaf/thallus/needle segments were placed on the upper side of a plastic grid that allowed natural air circulation above and below the segment.

The grid with the sample was placed on a laboratory weighing scale to measure the initial fresh mass (FM) of the sample, as well as the fresh mass during desiccation (FMDD). The sample segment remained on the laboratory scale for the entire desiccation period until the segment mass became constant, indicating it had reached dry mass (DM). This arrangement allowed the simultaneous evaluation of FW and ChlF since a fluorometer probe was fixed 0.5 cm above the sample segment for the entire measurement period.

The sample segments were desiccated at 23°C and 80% relative humidity. After desiccation, when all ChlF reached zero, the sample segments were transferred to an oven and dried at 80°C for 24 h to reach DM (measured on the analytical scale). Finally, the relative water content (RWC) values for the leaf/thallus/needle segments during the desiccation period (typically recorded at 30-min intervals) were calculated using the following formula:

$$RWC = (FMDD - DM) \times 100/(FMo - DM) \quad (1)$$

where FMDD is the FM of the sample recorded at any time during the desiccation period, DM is the DM of the sample, and FMo is the initial FM at the beginning of the experiment. The calculated RWC values were used to evaluate the desiccation-response curves of the ChlF related to PSII function and protective mechanisms, particularly NPQ.

Measurement of chlorophyll fluorescence: The ChlF of the evaluated species were measured using a *PAM 2500* fluorimeter (*Walz*, Effeltrich, Germany) following the NPQ induction/relaxation curve method. Measurements began after the samples were kept in the dark for 15 min to achieve a dark-adapted state. The minimum ChlF (F_0) and maximum ChlF (F_M) were then measured to calculate the maximum quantum yield of PSII (F_V/F_M, Eq. 2) and the ratio of minimum to maximum ChlF in the dark-adapted state.

For F_M measurements, a 0.8-s saturation pulse (SP) of 2,000 μmol(photon) m^{-2} s^{-1} PAR was used. The samples were then exposed to actinic light [670 μmol(photon) m^{-2} s^{-1}] for a period of 2 min 20 s. The actinic light period was selected relatively short because the results gained could be comparable to our previous study done in poikilohydric organisms, which used such a period. Moreover, we were interested in the initial sharp NPQ rise, which is driven by fast activated energy-dependent quenching (q_E). At the end of 2-min light period, the local maximum and/or initial steady-state level is reached. During this light period, saturation pulses were applied every 20 s to induce the maximum ChlF signal (F_M'), which was then used to calculate Φ_{PSII}, ETR, coefficient of photochemical quenching (q_P), and NPQ using the equations provided below.

A key advantage of this method is that it records a curvilinear (exponential) increase in NPQ while the sample is exposed to constant actinic light. The actinic light was then switched off for three minutes (dark period), and saturation pulses were applied every 20 s to measure the maximum ChlF (F_M'') and calculate NPQ values during the dark relaxation period.

ChlF was monitored using the *PamWin 3.0* software package (*H. Walz*, Germany) throughout the light and dark periods (*see* Kautsky kinetics in the *Supplement* – Fig. 1S), and the changes induced by sample desiccation were evaluated. From the curves, the maximum value

(ETR_{max}) and the slope of the relationship (parameter) were calculated using the built-in formulas in the *PAM 2500* fluorometer.

$$F_V/F_M = (F_M - F_0)/F_M \quad (2)$$

$$\Phi_{PSII} = (F_M' - F_t)/F_t \quad (3)$$

$$rETR = (PAR \times 0.84 \times \Phi_{PSII})/2 \quad (4)$$

$$NPQ = (F_M - F_M')/F_M' \quad (5)$$

$$\Phi_{NPQ} = (F_t - F_M')/(F_t - F_M) \quad (6)$$

$$q_P = (F_M' - F_t)/(F_M' - F_0') \quad (7)$$

where F_0 is the dark-adapted background ChlF, F_M is the maximum ChlF reached after an SP is applied in the dark-adapted state, F_M' is the maximum ChlF reached after an SP is applied in the light-adapted state (at the end of the light period), F_t is the ChlF recorded at the end of the light period, and PAR is the photosynthetically active radiation. F_0' was measured for the light-exposed sample during post-pulse illumination with far-red light.

NPQ induction and relaxation curves: The ETR and NPQ values for the light and dark periods were plotted against time. Mean curves for the two parameters were calculated for descending RWC classes (90–100%, 80–90%, 70–80%, 60–70%, 50–60%, 40–50%, 30–40%, 20–30%, 10–20%, and 0–10%). From the curves (*see* Fig. 1), the following parameters were calculated: (*1*) the initial slope of NPQ increase at the beginning of the actinic light period (α), (*2*) the ratio of decrease $(NPQ_{termin} - NPQ_{relax})/NPQ_{termin}$, (*3*) the slope of the initial decrease at the beginning of the dark relaxation period (β), and (*4*) NPQ_{relax}. Data forming the induction and relaxation parts of the curve were fitted by exponentials using the formula:

$$NPQ = y0 + a \times \exp(-b \times x) \quad (8)$$

where a, b, and y0 are coefficients, and x represents time in seconds, starting from zero at the beginning of the induction/relaxation part of the NPQ curve. Energy-dependent quenching (q_E), as well as photoinhibitory and state transition-related quenching (q_{I+T}), were calculated according to Ruban (2017) from ChlF data recorded for specific species at different RWCs as measured during gradual desiccation. The following formulae were used:

$$q_E = (F_M'' - F_M')/F_M' \quad (9)$$

$$q_I = (F_M - F_M')/F_M'' \quad (10)$$

where F_M'' is the maximum ChlF after the application of the SP at the end of the dark period (180 s after the actinic light was switched off), F_M' is the maximum ChlF reached after the application of the SP in the light-adapted state (at the end of the light period), and F_M is the maximum ChlF reached after the application of the SP in the dark-adapted state.

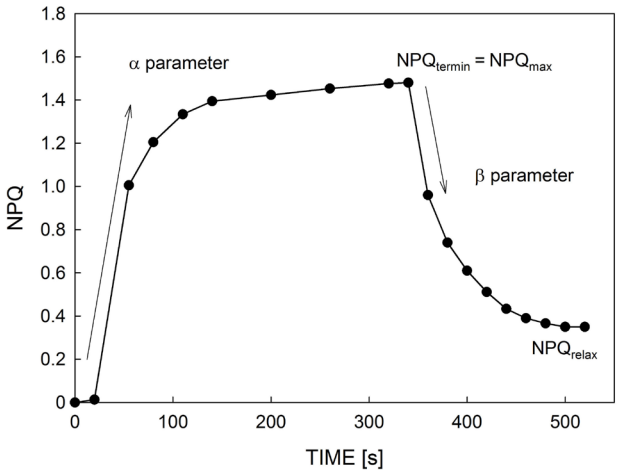

Fig. 1. Typical NPQ induction and relaxation curve with definitions of the parameters used in the study: NPQ recorded at the end of NPQ induction, that is, the terminal value of NPQ (here equal to the maximum value), α parameter – the slope of the initial part of NPQ induction, β parameter – the slope of the initial NPQ decrease at the beginning of the dark period (relaxation curve). The α and β parameters were calculated as ΔNPQ/Δtime(s).

Desiccation-response curves for F_V/F_M: For each of the evaluated species, F_V/F_M values were plotted against RWC, and the data points were fitted to an S-curve using the formula from *SigmaPlot v. 11* software (*Systat Software*, *Inc*., USA). From the S-curves, the following parameters were evaluated: (*1*) RWC_{init} (the RWC range at which F_V/F_M values did not show any substantial decrease during the initial phase of desiccation – phase I sensu Barták *et al.* 2016), (*2*) RWC_{50} (the RWC value at which F_V/F_M reaches half of its maximum value), and (*3*) RWC_{crit} (the RWC value at which F_V/F_M was fully limited and reached zero). Species-specific responses in the dehydration-induced decline in F_V/F_M were evaluated.

Statistical analysis: The effects of desiccation (expressed as RWC) on ChlF were evaluated through a one-way analysis of variance (*ANOVA*) using the *STATISTICA* software with P=0.05. The significance of the relationship between individual ChlF, as affected over the course of desiccation, was expressed on a heatmap.

Results

Desiccation-response curves for F_V/F_M: In all the evaluated species, F_V/F_M decreased with gradual desiccation from an RWC of 100% to 0%, showing species-specific curvilinear relationships (Fig. 2). RWC_{50} – the RWC at which F_V/F_M reaches 50% of its maximum value – is presented in Table 1, along with RWC_{50} for q_P. For F_V/F_M, individual species had RWC_{50} values ranging from 41% for *S. lycopersicum* to about 12.2% for *M. moschata*.

The critical RWC (RWC_{crit}), at which the samples approached complete dryness with an F_V/F_M of zero, was determined using a linear regression of the F_V/F_M data at an RWC below 15%. At RWC_{crit}, the F_V/F_M calculated from the fitted data was zero, indicating full inhibition of PSII-related photosynthetic processes. RWC_{crit} was species-specific, although it remained below 10% RWC.

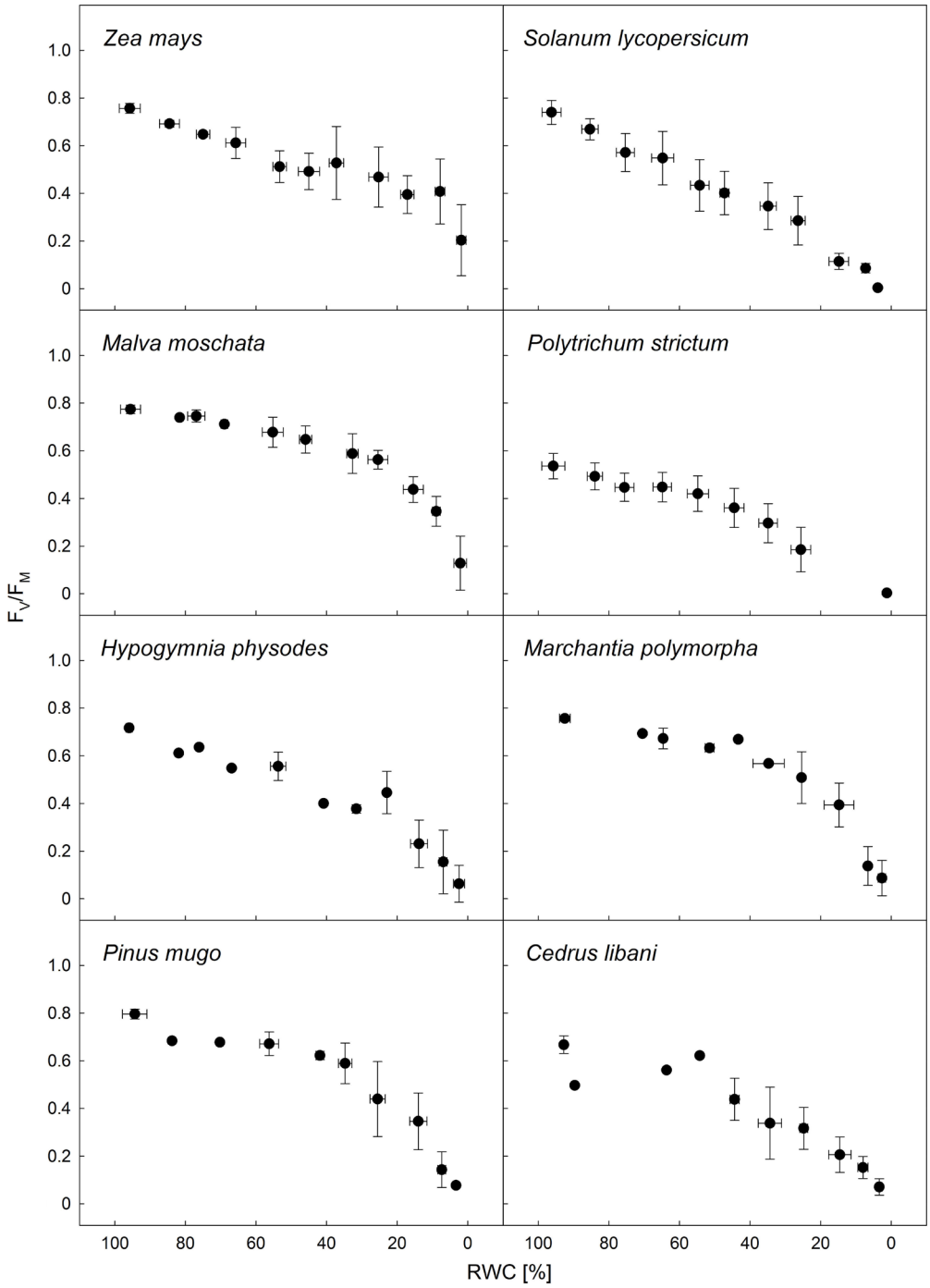

Fig. 2. Maximum quantum yield of photochemical processes in PSII (F_V/F_M) with its dependence on relative water content (RWC). The data points represent the mean of at least four replicates ± the standard deviation (SD).

The lowest RWC_{crit} occurred in poikilohydric *H. physodes* and *M. polymorpha*, as well as in a conifer (*C. libani*) and a C_3 plant (*M. moschata*). For all species, RWC_{50} and RWC_{crit} for q_P reached higher values than those for F_V/F_M (Table 1).

Effect of desiccation on slow Kautsky kinetics: Gradual desiccation led to a change in the shape of the slow Kautsky kinetics. The greater the water loss, the lower the ChlF values that formed the curve. Such desiccation-induced flattening of the Kautsky kinetics is shown in Fig. 3 for *H. physodes*. For species-specific changes in Kautsky kinetics and desiccation-induced shape changes, *see* Fig. 1S.

NPQ induction/relaxation curves and related parameters: In a fully hydrated state (RWC = 100%), the NPQ induction curves, regardless of their species-

Table 1. The relative water content (RWC) at which 50% of the maximum F_V/F_M and q_P values were reached (RWC_{50}) and the critical RWC (RWC_{crit}) at which F_V/F_M and q_P reached zero for each of the evaluated species. The data points represent the mean of at least four replicates ± the standard deviation (SD). Upper index characters indicate statistically significant difference. F_V/F_M – maximum quantum yield of photochemical processes in PSII for light-acclimated state; q_P – photochemical quenching.

Species	F_V/F_M		q_P	
	RWC_{50}	RWC_{crit}	RWC_{50}	RWC_{crit}
Zea mays	12.1 ± 0.9^{d}	7.1 ± 0.2^{b}	84.2 ± 10.1^{a}	22.1 ± 2.7^{a}
Solanum lycopersicum	41.0 ± 3.6^{a}	8.9 ± 0.4^{a}	34.6 ± 4.8^{b}	14.6 ± 2.0^{b}
Malva moschata	12.2 ± 0.3^{d}	2.1 ± 0.1^{d}	27.8 ± 2.2^{c}	5.2 ± 0.4^{e}
Polytrichum strictum	33.1 ± 2.8^{b}	8.5 ± 0.5^{a}	20.0 ± 3.0^{d}	11.1 ± 1.2^{bc}
Hypogymnia physodes	33.2 ± 0.5^{b}	1.6 ± 0.1^{d}	16.0 ± 1.4^{e}	3.0 ± 0.3^{f}
Marchantia polymorpha	18.3 ± 0.3^{c}	1.8 ± 0.1^{d}	39.9 ± 5.2^{b}	12.2 ± 1.8^{b}
Pinus mugo	20.0 ± 0.8^{c}	4.2 ± 0.2^{c}	38.2 ± 4.2^{b}	7.8 ± 0.9^{d}
Cedrus libani	36.2 ± 0.6^{b}	1.7 ± 0.1^{d}	45.8 ± 6.4^{b}	9.9 ± 1.2^{c}

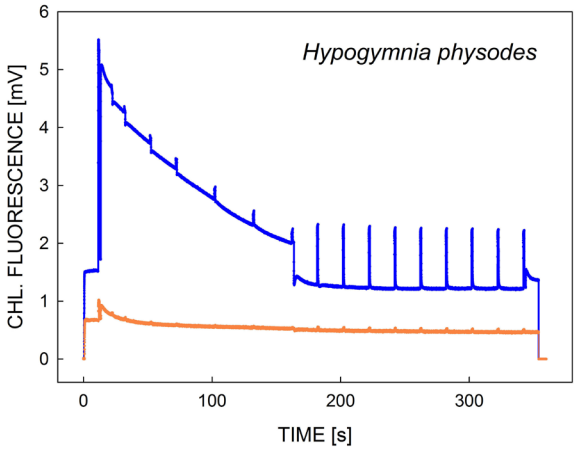

Fig. 3. Time characteristic of slow Kautsky kinetics for a fully hydrated thallus (*blue line*, RWC 100%) and a substantially desiccated thallus of *Hypogymnia physodes* (*orange line*, RWC 14%).

specific shapes, showed two general phenomena. In all the evaluated species, (*1*) a gradual increase in NPQ values was observed during the light period of measurement, reaching a maximum at the end after three minutes of illumination, and (*2*) the NPQ values forming the induction curve during the light period were almost exclusively at their highest with an RWC of 95% (except *M. moschata* and *H. physodes*) and then decreased as desiccation increased, eventually exhibiting a very low NPQ (below 0.2) at RWCs between 5 and 10%.

The shape of the NPQ induction curve during the light period of measurements was found to be species-specific. An exponential rise with a maximum (constant) value of NPQ reached at the end of the light period was most typical (*e.g.*, *S. lycopersicum*, *P. mugo*, *C. libani* at 95% RWC). However, some NPQ induction curves followed an S-curve (*e.g.*, *Z. mays*, *M. moschata* at 95% RWC) that was still slightly rising at the end of the light period of measurements.

The absolute value of NPQ recorded at the end of the light period (NPQ_{termin}) decreased as RWC decreased (Fig. 4). However, the shape of the relationship was species-specific: (*1*) a linear decrease (*C. libani*, *Z. mays*), (*2*) an exponential decrease (*S. lycopersicum*, *P. mugo*), and (*3*) an initial plateau followed by a decrease in NPQ at RWC below 60% (*M. moschata*), 50% (*P. strictum*), and 40% (*M. polymorpha*, *H. physodes*). Φ_{NPQ} decreased with decreasing RWC, showing a steady decline as RWC decreased from 100% to 20%, with a more pronounced drop below 20%.

During the dark relaxation period, NPQ values decreased exponentially for all evaluated species and RWC levels. In hydrated leaves/thalli/needles, the difference between NPQ_{max} and NPQ_{relax} (*see* Fig. 1S) was significantly higher than in samples exhibiting moderate drought stress, such as those with an RWC range of 30–50%. With severe desiccation, at an RWC of less than 15%, no substantial relaxation of NPQ values was observed after the decrease from NPQ_{max} to NPQ_{relax}, which had already reached extremely low values.

Apart from the relaxation-related decrease in NPQ values, the speed of the NPQ decrease (beta parameter) was generally found to be desiccation-dependent. The initial rate of NPQ decrease at the very beginning of the dark period was highest at an RWC of about 100% and decreased as the RWC decreased. Exponentials fitted through NPQ induction (light period) and relaxation (dark period) revealed that the y0, a and b parameters changed during sample desiccation (Table 4S, *Supplement*). For induction kinetics, the general trend was a decrease in y0 and an increase in a and b. For NPQ relaxation kinetics, y0 and a decreased with desiccation, while b showed irregular changes.

The relative decrease in NPQ during the relaxation period – that is, $(NPQ_{termin} - NPQ_{relax})/NPQ_{termin}$ – diminished as the degree of desiccation increased. The relationship between this parameter and RWC was species-specific, as the rates of decrease varied, particularly in the first phase of desiccation (a decrease in RWC from 100 to 60%). The rate of decrease was high for *S. lycopersicum* and *P. mugo*, while it was slower for the other evaluated species (*see* Fig. 5).

Quenching analysis: During sample desiccation from 100% to 0% RWC, q_P exhibited a species-specific decrease

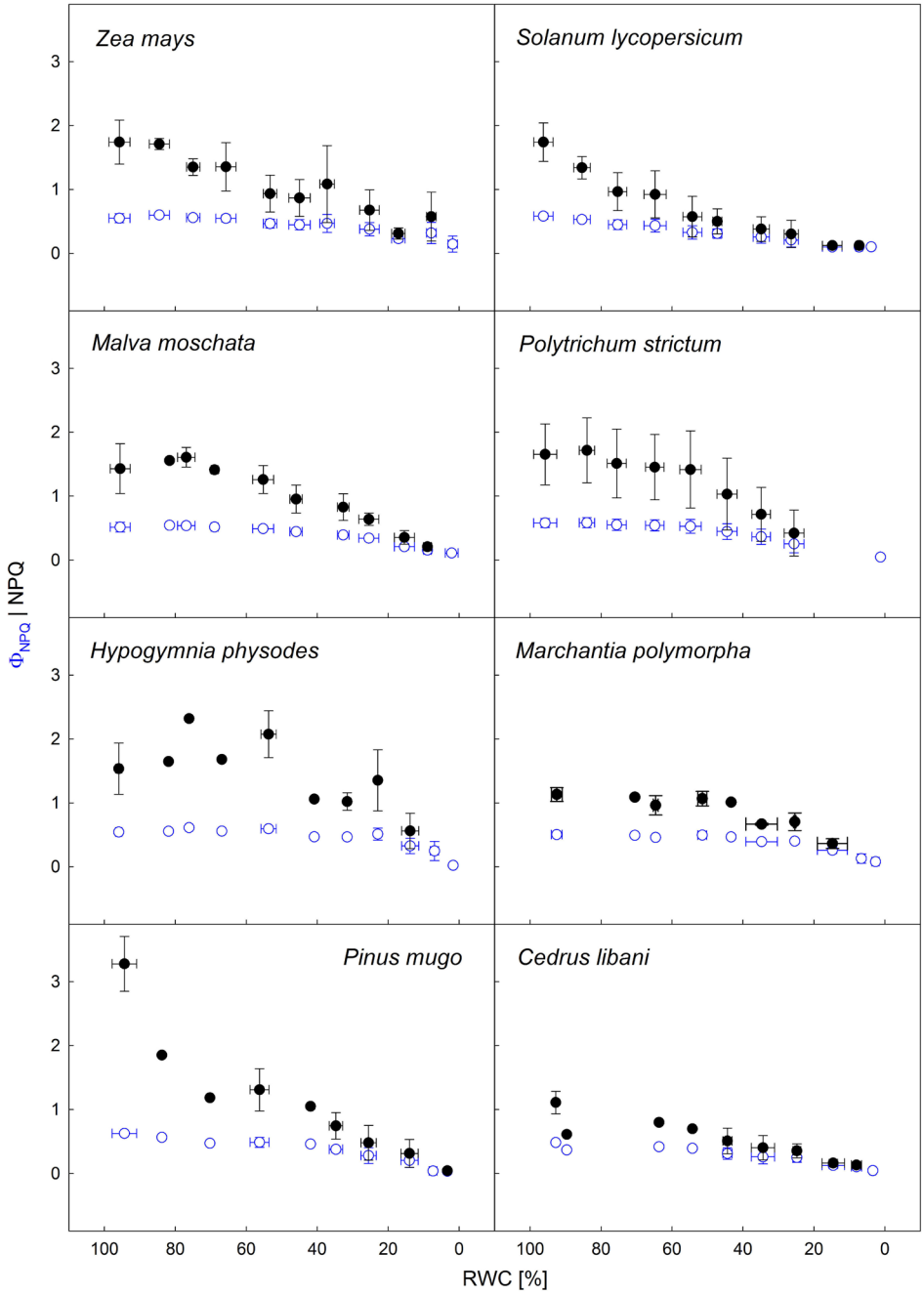

Fig. 4. The relationship between non-photochemical quenching (NPQ, values of NPQ_{termin} are presented), the quantum yield of non-photochemical quenching (Φ_{NPQ}), and relative water content (RWC) during desiccation. The means of the RWC classes (90–100%, 80–90%, 70–80%, 60–70%, 50–60%, 40–50%, 30–40%, 20–30%, 10–20% and 0–10%) ± the standard deviation (SD) are presented.

(Fig. 2S, *Supplement*). In *Z. mays* and *P. mugo*, q_P decreased gradually from the very beginning. In *S. lycopersicum*, *C. libani*, and *M. polymorpha*, the parameter remained relatively constant during the initial phase of desiccation, followed by a decrease towards zero q_P at an RWC of 0%.

Some samples showed an increase in q_P during the initial phase of desiccation, reaching maxima at an RWC of 70% (*M. moschata*), 50% (*H. physodes*), and even 30% (*P. strictum*). With continued desiccation, these three species exhibited a decrease towards zero q_P at an RWC of 0%.

The share of q_E and q_{I+T} that drives NPQ was affected by progressive desiccation (Fig. 6). As the evaluated samples moved towards severe levels of desiccation, the q_{I+T} component increased dramatically, typically at RWCs below 20%. Species-specific differences in the q_E and q_{I+T} components were apparent even at high RWCs at the beginning of desiccation treatment. The highest values

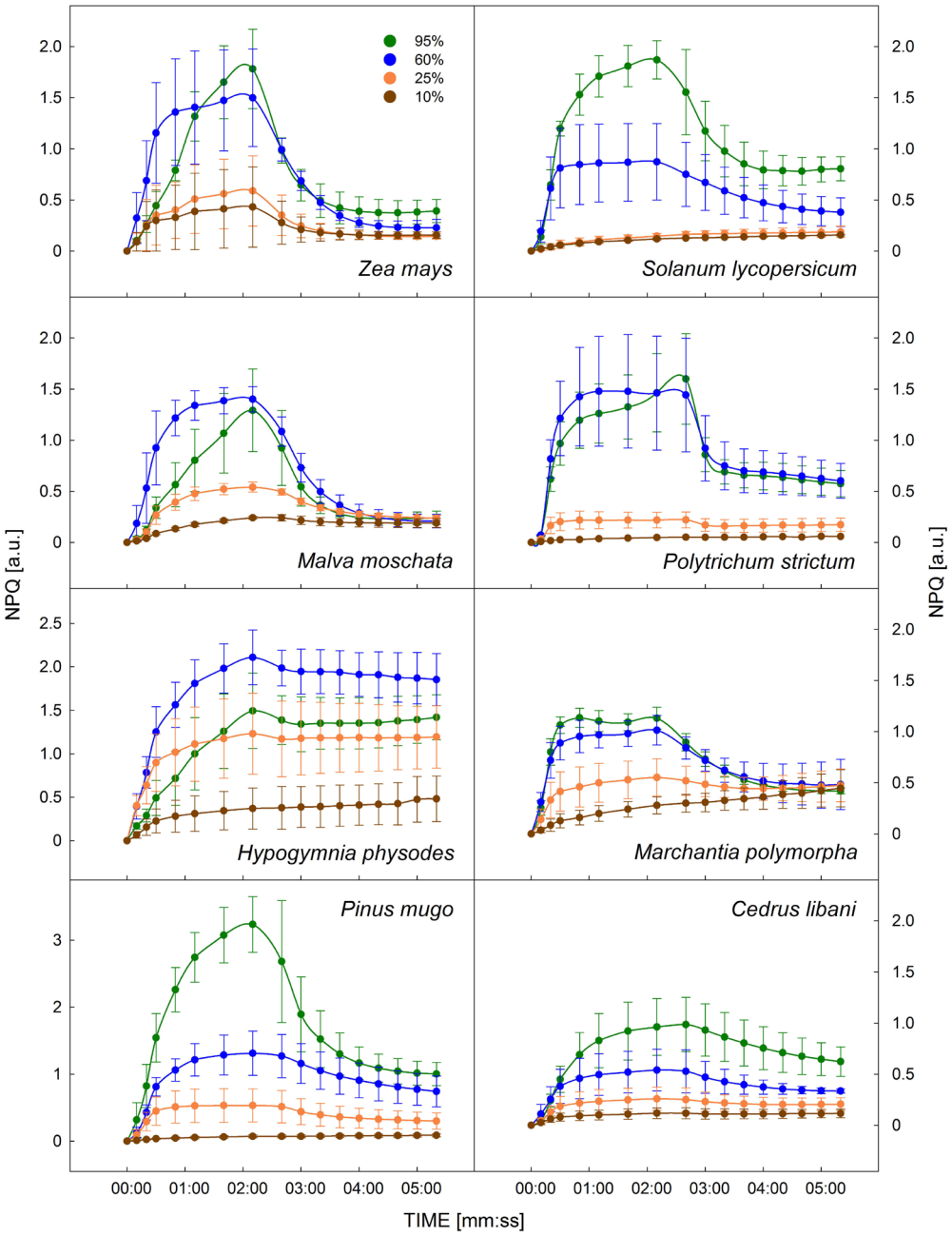

Fig. 5. The non-photochemical quenching (NPQ) induction/relaxation curves for the evaluated species recorded for selected RWC classes (95%, 60%, 25%, 10%). The data points represent means of ten replicates ± standard deviations.

of q_E and the lowest values of q_{I+T} were found for *Z. mays* and *M. moschata*, while a dominant proportion of q_I was found for *H. physodes* at an RWC of 100%.

At a medium-to-severe stage of desiccation (RWC of 60–80%), a decrease in the proportion of q_E was observed, accompanied by an increase in q_{I+T}. Across all evaluated species, the relative share of q_E and q_{I+T} differed at an RWC of 60%. *Z. mays* and *M. moschata* maintained a high share of q_E (above 50% of total NPQ), while the q_{I+T} level prevailed in the other evaluated species.

At an RWC below 20%, q_{I+T} accounted for the vast majority (95–100%) of NPQ in *H. physodes*, *C. libani*, and *S. lycopersicum*, while q_E was either significantly diminished (less than 5% of total NPQ) or absent. Even at an RWC close to the critical point, *Z. mays* maintained around 20% q_E of total NPQ. The relative decline of NPQ from NPQ_{max} to NPQ_{relax} is shown in Fig. 7.

Discussion

Desiccation response curves for F_V/F_M and q_P: Desiccation-induced decrease in F_V/F_M and q_P is reported for initial stages (stomata-controlled) as well as severe stress accompanied by extremely low water content in leaves (Skotnica *et al.* 2000). In our study, F_V/F_M decreased due to

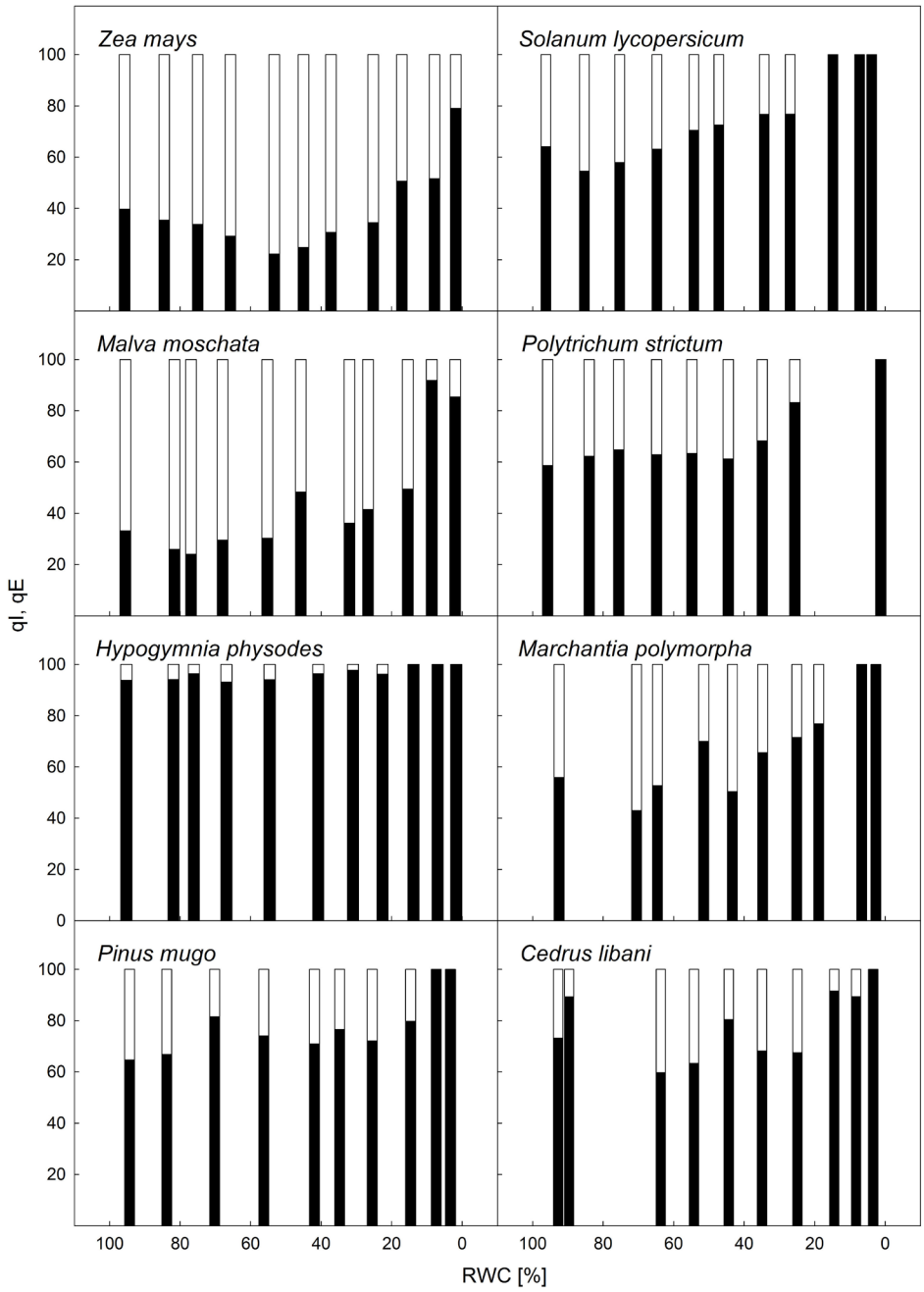

Fig. 6. Relative proportion of energy-dependent quenching (q_E) and photoinhibitory quenching (q_I) evaluated for relative water content (RWC) during sample desiccation from an RWC of 100% to 0% (dry state). Together, *the black* and *white columns* represent the overall NPQ.

gradual desiccation, following an exponential or S-curve species-specific decline. Species-specificity is supported by Trueba *et al.* (2019), who reported a great variety of exponential/sigmoidal F_V/F_M to RWC relationships in ten species of herbs and trees. A species-specific difference relates to (*1*) the point (RWC) at which a substantial decrease of F_V/F_M starts, (*2*) the rate of F_V/F_M decline with further RWC decrease, as well as (*3*) the rate of the most rapid F_V/F_M decline. The critical point (RWC) at which zero was reached was also species-specific (Table 1); however, consistent with a previous study on *Arabidopsis*, which showed declines of F_V/F_M at a very similar RWC threshold (Woo *et al.* 2008). Critical RWC values for F_V/F_M were very low, which might be attributed to the fact that F_V/F_M was the 'last' ChlF parameter responding to severe dehydration, while the other parameters responded more sensitively to dehydration-induced damage to chloroplasts. This might be associated with either substantial loss of hydraulic function or full hydraulic disruption of leaf cells and chloroplasts (Cardoso *et al.* 2018). In poikilohydric

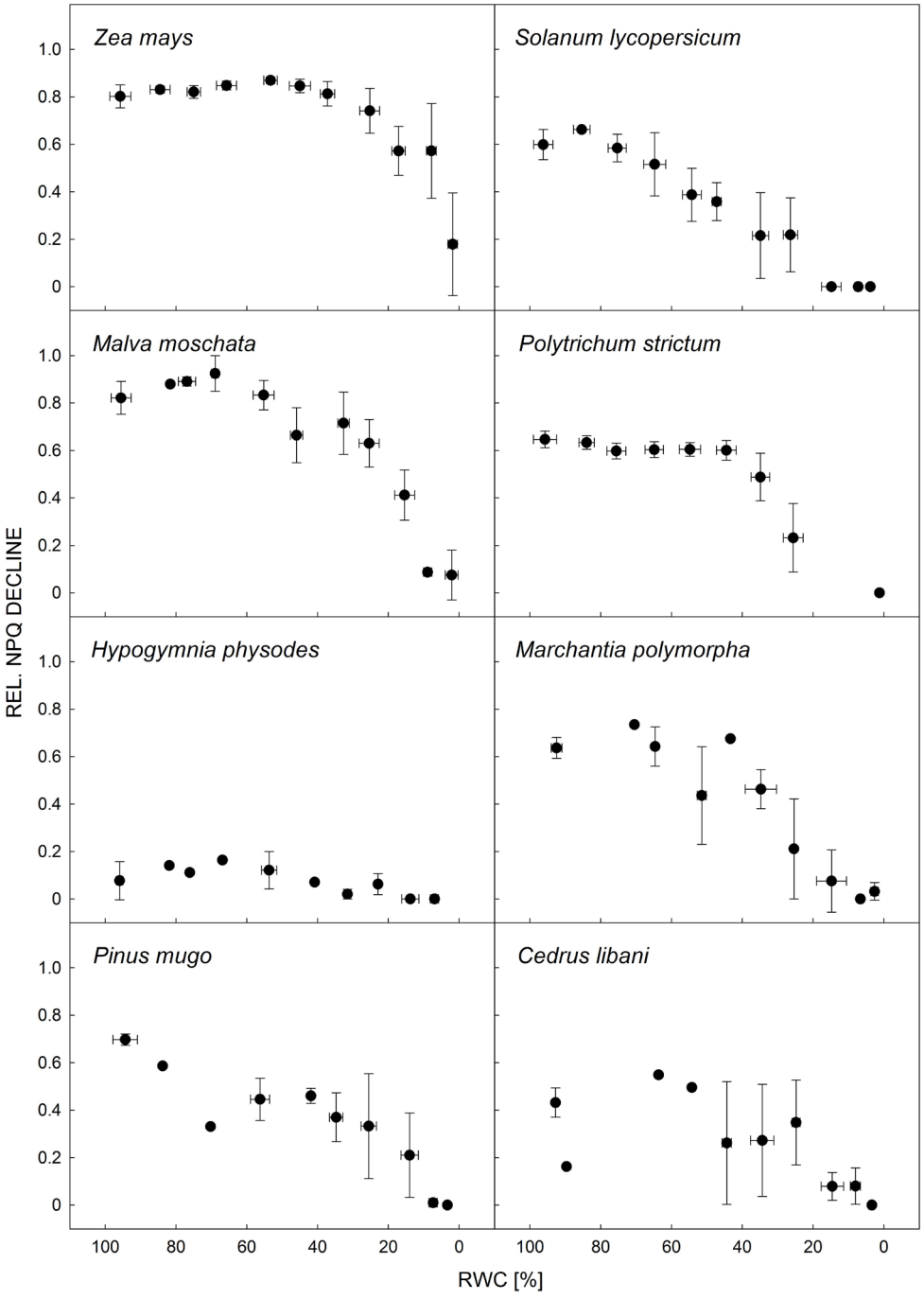

Fig. 7. The relative decline in non-photochemical quenching from NPQ_{termin} to NPQ_{relax} and their dependence on the decline in relative water content (RWC) during the desiccation of the evaluated samples. The data points represent the mean ± standard deviation (SD).

autotrophs (*P. strictum*, *H. physodes*, *M. polymorpha*), the F_V/F_M to RWC relationship showed a typical S-curve, similar to previous evidence gained for lichens (Barták *et al.* 2015, 2021). The RWC at which the most rapid F_V/F_M decline occurred was comparable to the data of Nayaka and Saxena (2014), *i.e.*, RWC of 20–30%.

The desiccation-induced decrease in F_V/F_M was caused by both a decrease in F_M and F_0, similarly to Khapte *et al.* (2024). However, F_0 decreased in lower rate than F_M. Faster desiccation-induced decrease in F_M than F_0 is associated with stress-induced damage and loss of integrity of PSII (Cardoso *et al.* 2018). Desiccation-induced decrease in F_V/F_M is reported even for drought-tolerant conifers, such as *e.g.*, *Pinus radiata* exposed to drought stress (Mena-Petite *et al.* 1999). Increases in F_0 (relative to F_M) represent a plant response to various stressors, such as high temperature (Zivcak *et al.* 2010) and uncouplers such as DCMU (Evdokimova *et al.* 2013).

The decrease in q_P was species-specific and not observed in some species during the initial phase of desiccation (RWC decline from 100 to 40%), where rather an increase in q_P was apparent. Such q_P behaviour might be associated with the contribution of specific photosynthetic processes affecting q_P during RWC lowering.

One factor influencing q_P is PAR. It is well established that when PAR is low, the photosynthetic electron transport is limited, and therefore, no significant effects on q_P are observed (Lawlor and Cornic 2002). With an increase in PAR, the extent of desiccation-induced decrease in q_P increases, accompanied by a decrease in F_V/F_M and effective quantum yield of PSII chemistry at light-acclimated state, as shown by Liu *et al.* (2012) for *Zea mays*. In general, q_P is typically negatively affected by severe but not mild drought stress (Tezara *et al.* 1999). At low RWC, q_P is limited by the direct dehydration effect on Rubisco, which becomes increasingly hydrolysed, leading to a decrease in its catalytic activity and enzyme affinity for CO_2 (reviewed by Zlatev and Lidon 2012).

Shape of NPQ induction /relaxation curve: The shapes of the NPQ induction curves at an RWC of 100% were species-specific, as shown by Beckett *et al.* (2021b), who investigated NPQ in ten lichen species and distinguished three categories: (*1*) a gradual increase in NPQ with a maximum constant value found at the end of the light period, (*2*) a rapid increase in NPQ with the maximum value reached before the end of the light period, followed by a slight decrease, and (*3*) a gradual increase with a rise in NPQ that had not reached a plateau at the end of the light period. Our data (Fig. 5) well correspond to the above-described case (*1* for *M. polymorpha*, *P. mugo*, *3* for *Z. mays*, *P. strictum*, *C. libani*, *H. physodes*), and the shape of NPQ curves might be classified as a typical high-light one, since the experimental species did not exhibit a low light-dependent decline in NPQ at the end of the light period (Ramakers *et al.* 2025).

As desiccation progressed, the NPQ induction curves changed in all examined species, showing lower absolute NPQ values as desiccation intensified. This observation aligns with a study of Mishra *et al.* (2024), focused on *Chorisodontium aciphyllum* moss: NPQ values at the end of the light period decreased with thallus desiccation.

At RWC below 80%, the experimental plants showed a gradual decrease in NPQ and Φ_{NPQ} with further desiccation (Fig. 4), similar to the data reported by Špundová *et al.* (2024) for *Nicotiana tabacum* and *Hordeum vulgare.* In the study, NPQ was measured after 1-minute exposure of leaves to light (*cf.* 2 min in our experiment). In our data recorded during desiccation, NPQ and Φ_{NPQ} were positively linearly correlated, suggesting that the two parameters are coupled, similarly to the study by Singh *et al.* (2022), who reported a high correlation for *Z. mays* plants under drought stress. Moreover, the NPQ and Φ_{NPQ} values responded to desiccation-induced inhibition of PSII (Fig. 2, F_V/F_M), similarly to Zait *et al.* (2024) demonstrated the relation for six vascular agricultural plants in response to desiccation.

Lichens show higher NPQ than rapidly growing organisms, enabling safe dissipation of excess light during short-term high-light episodes (Demmig-Adams *et al.* 2014). In *H. physodes*, NPQ_{max} first increased during desiccation (*vs*. wet state, RWC of 95%, Fig. 5), then declined under severe desiccation (RWC ~25–10%). A similar pattern was reported for desiccating *Parmelia quercina* by Calatayud *et al.* (1997). The rise in NPQ in moderately dehydrated lichen thalli likely reflects enhanced protection of PSII from overenergisation and ROS formation.

Fast thermal dissipation in desiccating lichens occurs in LHC pigment–protein complexes, preventing the PSII core overenergisation (Heber 2008). This leads to the formation of reversibly inactive PSII centres that act as a photoprotective mechanism (Heber *et al.* 2010).

The relative decline of NPQ (Fig. 7) suggests a threshold where NPQ is negatively affected and impaired. In most experimental species (except *S. lycopersicum*), NPQ decreased markedly when RWC fell below ~40–30%.

The initial slope of the NPQ induction curves (α) increased with desiccation across, consistently with Mishra *et al.* (2024), who observed a gradual increase as RWC declined from 100% to 0%. However, they also reported a desiccation-induced increase in α followed by a decrease when RWC dropped 50%.

The initial rate of NPQ dark relaxation (β) changed with RWC in all species, becoming less steep as desiccation intensified, indicating impaired PSII function. This agrees with findings for other stressors limiting NPQ dark relaxation, such as high temperature (Permann *et al.* 2022), photoinhibition of PSII (Kress and Jahns 2017), and UV-B stress (Xue *et al.* 2022). Similar β changes occur in *A. thaliana* (npq4) mutants lacking the PsbS protein essential for NPQ activity (Takahashi *et al.* 2009) and *Physcomitrium patens* mutants deprived of chlorophyll *b* (Zhang *et al.* 2023).

Overall, desiccation-driven changes in α, β, and derived parameters (y0, a, b) indicate stress effects and their usefulness as drought indicators.

NPQ components in response to the decrease in RWC: The rapid induction and relaxation of NPQ – within seconds to minutes – is driven by q_E, activated by ΔpH, the trans-thylakoidal gradient linked to protonation of the lumen (Zaks *et al*. 2013). Other mechanisms, such as photoinhibitory quenching (q_I), relax more slowly, over minutes to hours (Murchie and Niyogi 2011). This matches data for *Z. mays* and *M. moschata* during RWC decline from 100% to ~50%, where q_E dominates NPQ. Similarly, Itam *et al*. (2024) showed in *Poa pratensis* and *Lolium perenne* under prolonged drought (240 h) that q_E contributed more than q_I during early stress (0–120 h), followed by a similar decline in q_E, q_I, and NPQ under severe stress (120–240 h). In our data, however, as desiccation intensifies (RWC ~50% to 0%), q_I prevails over q_E.

In poikilohydric autotrophs (*H. physodes*) and conifers (Fig. 6), q_I remains the main NPQ component across the full RWC range, unlike vascular plants. During

early desiccation, q_E still plays a key role *via* (*1*) ΔpH-driven deepoxidation of violaxanthin to zeaxanthin, which quenches PSII excitation energy, and (*2*) the PSII protein PsbS (Li *et al*. 2004). NPQ induction/relaxation studies show faster induction and higher NPQ with PsbS overexpression than in control *A. thaliana* (Demmig-Adams and Adams 2006).

Fast NPQ induction also involves pseudocyclic electron flow *via* flavodiiron proteins, which transfer electrons to oxygen (Gerotto *et al.* 2016). Desiccation-related changes in PSII and NPQ increase plant sensitivity to stresses such as excess light (Wang *et al.* 2018). In vascular plants, desiccation and high light often co-occur, causing stronger photoinhibition than single stresses.

In poikilohydric organisms, nonactive reaction centres and three mechanisms of excess energy dissipation occur during moss rehydration (Heber *et al.* 2006a,b; Yamakawa *et al*. 2012). These processes prevent photooxidation of PSII and appear as increased NPQ in desiccating mosses, along with decreased F_V/F_M and Φ_{PSII} (Giudici 2021).

Relationship between chlorophyll fluorescence parameters: Our data indicate some general trends, for example, a desiccation-induced decrease in NPQ and Φ_{NPQ} (*see* Fig. 4). The pattern of NPQ and Φ_{NPQ} change with the RWC decrease, however, differed between species, showing either a gradual decrease (such as in *S. lycopersicum* and conifers, *see* Fig. 4) or a more complex response. In some cases (*Z. mays*, *M. moschata*, *H. physodes*, *P. mugo*), the dehydration response curves differed between NPQ and Φ_{NPQ}. It is because of the different contributions of $\Phi_{f,D}$, since $NPQ = \Phi_{NPQ}/\Phi_{f,D}$ (Lazár 2015). The author reported that the same numerical NPQ value may be obtained for different values of Φ_{NPQ} and $\Phi_{f,D}$, which should be taken into consideration in the studies focused on non-photochemical quenching.

For most evaluated species, NPQ_{termin} plotted against RWC showed either a slight increase or no change during early desiccation, followed by a decrease at RWCs below about 80%. This agrees with Proctor *et al.* (2007), who reported an initial increase in NPQ, followed by a decrease in NPQ for RWC intervals from 50% to 100% and from 0% to 50% in the moss *Polytrichum formosum*. This pattern might reflect the activation of a protective mechanism (an increase in NPQ) during phase I, when F_V/F_M remains high and declines slowly. In phase II (more pronounced desiccation), NPQ decreases alongside a rapid loss of PSII efficiency as F_V/F_M drops. This explanation might be supported by the data recorded for rewetted moss, *Sanionia uncinata*, in which the peak NPQ was achieved when the F_V/F_M values reached their maximum after 24 h of rewetting (Orekhova and Hájek 2022). The protection of mosses – specifically their PSII-related processes – against desiccation effects encompasses several mechanisms, including dithiothreitol activity, thermal dissipation, and the accumulation of radicals acting as quenchers of excitation energy in RC of PSII (Yamakawa *et al.* 2012). Underlying mechanisms in chloroplasts are (*1*) protonation of thylakoid proteins (active in hydrated mosses); (*2*) exciton migration towards the light-harvesting complexes (LHCs), where fast thermal dissipation takes place, and (*3*) reversible photoaccumulation of radicals. The same author (Yamakawa and Itoh 2013) classifies NPQ in desiccating poikilohydric plants as d-NPQ, in contrast to the non-photochemical quenching induced by high light (abbreviated l-NPQ). In our experiment, the dominant share of d-NPQ from the total NPQ could be expected in moss *P. strictum* as well as a lichen (*H. physodes*), and a liverwort (*M. polymorpha*), because the desiccation happened under low-light conditions (*see* Materials and methods). However, an interaction between d-NPQ and l-NPQ could be expected during the final phases of thallus dehydration.

Concluding remarks: The lichen (*H. physodes*) and liverwort (*M. polymorpha*) evaluated in this study showed very low RWC_{crit} values, indicating high tolerance of their primary photosynthetic processes – F_V/F_M in particular – to desiccation. Numerous studies have focused on the mechanisms of desiccation tolerance in poikilohydric autotrophs (lichens, mosses, liverworts). These mechanisms include the production of large quantities of polyols and oligogalactolipids, the presence of a potent antioxidant system, lipid remodelling, changes at an ultrastructural level, as well as physiological responses such as NPQ and its components. Recent studies of poikilohydric organisms have even started to apply NPQ induction/relaxation kinetics in both wild-type and mutant forms to identify different quenching sites within the LHCII–PSII complex, as shown for *Physcomitrella patens* (Carbonera *et al.* 2012). Numerous methods exploiting ChlF have been applied to mosses to evaluate their desiccation-induced NPQ – for a review, *see* Morales-Sánchez *et al.* (2022). A recent study suggests combining experimental protocols, including ChlF, to assess desiccation tolerance in mosses. Our results for *P. strictum* suggest that NPQ induction/relaxation curves could be one of these approaches.

The vascular plants used in our study had higher RWC_{crit} values, indicating that they can cope with severe water loss from leaf tissue (below 40% RWC) only to a limited extent. Primary photosynthetic processes (F_V/F_M and Φ_{PSII}) remain active at such low RWC levels; however, gas exchange and photosynthetic CO_2 fixation may be strongly or fully limited. Therefore, future studies focusing on the effects of severe drought stress on photosynthesis in vascular plants should utilise both ChlF and gas-exchange methods to evaluate the relationship between primary and secondary photosynthetic processes, along with their limitations through stomatal conductance and reduced transpiration rates during leaf desiccation.

Moreover, follow-up studies should take measurements from (a) intact leaves, (b) detached leaves or (c) small-area leaf segments (as done in this study) to evaluate the effect of stomatal regulation of water loss in (a) and (b), and for (c) the loss of water from leaf cross-section margins or a similar simplified system.

Analysis of the NPQ induction/relaxation curves showed that the parameters derived in this study [α, β, $(NPQ_{termin} - NPQ_{relax})/NPQ_{termin}$, NPQ_{relax}] may serve,

alongside traditional parameters derived from the ETR light-response curve, as indicators of desiccation stress in a range of photosynthesising organisms – from poikilohydric lichens and mosses to crops and conifers. The analysis of NPQ induction/relaxation curves provides insights into protective mechanisms activated during varying degrees of desiccation and their involvement in PSII functioning.

In vascular plants, NPQ induction/relaxation kinetics are recommended for studies focusing on drought stress effects within an RWC range of 100 to 40%. The lower limit represents a state at which Φ_{PSII} approaches zero due to low leaf water content. If RWC falls below 60% (Kalariya *et al.* 2015) or 40% (as shown in this study for *Z. mays* and *M. moschata*), it leads to irreversible changes in the photosynthetic apparatus and leaf physiology. The low limit of about 40% RWC aligns with findings for drought-resistant mutations, as demonstrated in wheat (le Roux *et al.* 2021). If the low RWC limit is reached and maintained for several days, physiological processes in the leaf may not recover from the wilting point, even if the water supply to the leaf is restored.

References

Acebron K., Matsubara S., Jedmowski C. *et al.*: Diurnal dynamics of nonphotochemical quenching in *Arabidopsis npq* mutants assessed by solar-induced fluorescence and reflectance measurements in the field. – New Phytol. **229**: 2104-2119, 2020.

Banks J.A.: Chlorophyll fluorescence as a tool to identify drought stress in Acer genotypes. – Environ. Exp. Bot. **155**: 118-127, 2018.

Barboričová M., Filaček A., Mlynáriková Vysoká D. *et al.*: Sensitivity of fast chlorophyll fluorescence parameters to combined heat and drought stress in wheat genotypes. – Plant Soil Environ. **68**: 309-316, 2022.

Barták M., Hájek J., Halıcı M.G. *et al.*: Resistance of primary photosynthesis to photoinhibition in antarctic lichen *Xanthoria elegans*: photoprotective mechanisms activated during a short period of high light stress. – Plants-Basel **12**: 2259, 2023.

Barták M., Hájek J., Orekhova A. *et al.*: Inhibition of primary photosynthesis in desiccating antarctic lichens differing in their photobionts, thallus morphology, and spectral properties. – Microorganisms **9**: 818, 2021.

Barták M., Hazdrová J., Skácelová K., Hájek J.: Dehydration-induced responses of primary photosynthetic processes and spectral reflectance indices in Antarctic *Nostoc commune*. – Czech Polar Rep. **6**: 87-95, 2016.

Barták M., Trnková K., Hansen E.S. *et al.*: Effect of dehydration on spectral reflectance and photosynthetic efficiency in *Umbilicaria arctica* and *U. hyperborea*. – Biol. Plantarum **59**: 357-365, 2015.

Beckett R., Minibayeva F., Solhaug K., Roach T.: Photoprotection in lichens: adaptations of photobionts to high light. – Lichenologist **53**: 21-33, 2021a.

Beckett R.P., Minibayeva F.V., Mkhize K.W.G.: Shade lichens are characterized by rapid relaxation of non-photochemical quenching on transition to darkness. – Lichenologist **53**: 409-414, 2021b.

Calatayud A., Deltoro V.I., Barreno E., del Valle-Tascon S.: Changes *in vivo* chlorophyll fluorescence quenching in lichen thalli as a function of water content and suggestion of zeaxanthin-associated photoprotection. – Physiol. Plantarum **101**: 93-102, 1997.

Carbonera D., Gerotto C., Posocco B. *et al.*: NPQ activation reduces chlorophyll triplet state formation in the moss *Physcomitrella patens*. – BBA-Bioenergetics **1817**: 1608-1615, 2012.

Cardoso A.A., Brodribb T.J., Lucani C.J. *et al.*: Coordinated plasticity maintains hydraulic safety in sunflower leaves. – Plant Cell Environ. **41**: 2567-2576, 2018.

Dalal V.K., Tripathy B.C.: Water-stress induced downsizing of light-harvesting antenna complex protects developing rice seedlings from photo-oxidative damage. – Sci. Rep.-UK **8**: 5955, 2018.

Demmig-Adams B., Adams III W.W.: Photoprotection in an ecological context: the remarkable complexity of thermal energy dissipation. – New Phytol. **172**: 11-21, 2006.

Demmig-Adams B., Koh S.-C., Cohu C.M. *et al.*: Non-photochemical fluorescence quenching in contrasting plant species and environments. – In: Demmig-Adams B., Garab G., Adams W.W., Govindjee (ed.): Non-Photochemical Quenching and Energy Dissipation in Plants, Algae and Cyanobacteria. Advances in Photosynthesis and Respiration. Vol. 40. Pp. 531-552. Springer, Dordrecht 2014.

Evdokimova O.V., Kabashnikova L.F., Savchenko G.E.: Biogenesis of photosynthetic apparatus under the inhibition of energy processes in de-etiolated seedlings of barley (*Hordeum vulgare* L.). – Biochemistry-Moscow **7**: 148-156, 2013.

Flexas J., Medrano H.: Drought-inhibition of photosynthesis in C_3 plants: stomatal and non-stomatal limitations revisited. – Ann. Bot.-London **89**: 183-189, 2002.

Gerotto C., Alboresi A., Meneghesso A. *et al.*: Flavodiiron proteins act as safety valve for electrons in *Physcomitrella patens*. – PNAS **113**: 12322-12327, 2016.

Giudici G.N.M.: Combined chlorophyll fluorescence techniques to study environmental impact on the mountain moss *Polytrichum commune*. – Czech Polar Rep. **11**: 161-173, 2021.

Gotarkar D., Doran L., Burns M. *et al.*: High-throughput analysis of non-photochemical quenching in crops using pulse amplitude modulated chlorophyll fluorometry. – J. Vis. Exp. **185**: e63485, 2022.

Granda E., Camarero J.J.: Drought reduces growth and stimulates sugar accumulation: new evidence of environmentally driven non-structural carbohydrate use. – Tree Physiol. **37**: 997-1000, 2017.

Hazrati S., Tahmasebi-Sarvestani Z., Modarres-Sanavy S.A.M. *et al.*: Effects of water stress and light intensity on chlorophyll fluorescence parameters and pigments of *Aloe vera* L. – Plant Physiol. Biochem. **106**: 141-148, 2016.

Heber U., Bilger W., Shuvalov V.A.: Thermal energy dissipation in reaction centres and in the antenna of photosystem II protects desiccated poikilohydric mosses against photo-oxidation. – J. Exp. Bot. **57**: 2993-3006, 2006a.

Heber U.: Photoprotection of green plants: a mechanism of ultra-fast thermal energy dissipation in desiccated lichens. – Planta **228**: 641-650, 2008.

Heber U., Bilger W., Türk R., Lange O.L.: Photoprotection of reaction centres in photosynthetic organisms: mechanisms of thermal energy dissipation in desiccated thalli of the lichen *Lobaria pulmonaria*. – New Phytol. **185**: 459-470, 2010.

Heber U., Lange O.L., Shuvalov V.A.: Conservation and dissipation of light energy as complementary processes: homoiohydric and poikilohydric autotrophs. – J. Exp. Bot. **57**: 1211-1223, 2006b.

Hoegh-Guldberg O., Jacob D., Taylor M. *et al.*: Impacts of 1.5°C global warming on natural and human systems. – In: Masson-Delmotte V., Zhai P., Pörtner H.-O. *et al.* (Ed.): Global

warming of 1.5°C. An IPCC Special Report on the impacts of global warming of 1.5°C above pre-industrial levels and related global greenhouse gas emission pathways, in the context of strengthening the global response to the threat of climate change, sustainable development, and efforts to eradicate poverty. Pp. 175-312. Cambridge University Press, Cambridge-New York 2018.

Ikeuchi M., Sato F., Endo T.: Allocation of absorbed light energy in photosystem II in NPQ mutants of *Arabidopsis*. – Plant Cell Physiol. **57**: 1484-1494, 2016.

Itam M., Hall D., Kramer D., Merewitz E.: Early detection of Kentucky bluegrass and perennial ryegrass responses to drought stress by measuring chlorophyll fluorescence parameters. – Crop Sci. **64**: 1015-1026, 2024.

Kalariya K.A., Singh A.L., Chakraborty K. *et al.*: Relative water content as an index of permanent wilting in groundnut under progressive water deficit stress. – Electron. J. Environ. Sci. **8**: 17-22, 2015.

Khapte P.S., Changan S.S., Kumar P. *et al.*: Deciphering desiccation tolerance in wild eggplant species: insights from chlorophyll fluorescence dynamics. – BMC Plant Biol. **24**: 702, 2024.

Kitao M., Yasuda Y., Kodani E. *et al.*: Integration of electron flow partitioning improves estimation of photosynthetic rate under various environmental conditions based on chlorophyll fluorescence. – Remote Sens. Environ. **254**: 112273, 2021.

Kress E., Jahns P.: The dynamics of energy dissipation and xanthophyll conversion in *Arabidopsis* indicate an indirect photoprotective role of zeaxanthin in slowly inducible and relaxing components of non-photochemical quenching of excitation energy. – Front. Plant Sci. **8**: 2094, 2017.

Lawlor D.W., Cornic G.: Photosynthetic carbon assimilation and associated metabolism in relation to water deficits in higher plants. – Plant Cell Environ. **25**: 275-294, 2002.

Lazár D.: Parameters of photosynthetic energy partitioning. – J. Plant Physiol. **175**: 131-147, 2015.

le Roux M.-S.L., Burger N.F.V., Vlok M. *et al.*: EMS derived wheat mutant BIG8-1 (*Triticum aestivum* L.) – a new drought tolerant mutant wheat line. – Int. J. Mol. Sci. **22**: 5314, 2021.

Li X.P., Gilmore A.M., Caffarri S. *et al.*: Regulation of photosynthetic light harvesting involves intrathylakoid lumen pH sensing by the PsbS protein. – J. Biol. Chem. **279**: 22866-22874, 2004.

Li X.-P., Müller-Moulé P., Gilmore A.M., Niyogi K.K.: PsbS-dependent enhancement of feedbackde-excitation protects photosystem II from photoinhibition. – PNAS **99**: 15222-15227, 2002.

Liu M., Qi H., Zhang Z.P. *et al.*: Response of photosynthesis and chlorophyll fluorescence to drought stress in two maize cultivars. – Afr. J. Agr. Res. **7**: 4751-4760, 2012.

Lu H.B., Qiao Y.M., Gong X.C. *et al.*: Influence of drought stress on the photosynthetic characteristics and dry matter accumulation of hybrid millet. – Photosynthetica **53**: 306-311, 2015.

Marchin R.M., Backes D., Ossola A. *et al.*: Extreme heat increases stomatal conductance and drought-induced mortality risk in vulnerable plant species. – Glob. Change Biol. **28**: 1133-1146, 2022.

Mena-Petite A., Duñabeitia M.K., Gonzalez-Moro B. *et al.*: Sequential effects of acidic precipitation and drought on water relations of *Pinus radiata* seedlings. – J. Plant Physiol. **155**: 93-100, 1999.

Meng L.L., Song J.F., Wen J. *et al.*: Effects of drought stress on fluorescence characteristics of photosystem II in leaves of *Plectranthus scutellarioides*. – Photosynthetica **54**: 414-421, 2016.

Mishra K.B., Rosputimský M., Grieš M., Puhovkin A.: Photoprotective mechanisms activated in Antarctic moss *Chorisodontium aciphyllum* during desiccation. – Czech Polar Rep. **14**: 1-9, 2024.

Mkhize K., Minibayeva F., Beckett R.: Adaptions of photosynthesis in sun and shade in populations of some Afromontane lichens. – Lichenologist **54**: 319-329, 2022.

Morales-Sánchez J.Á., Mark K., Souza J.P.S., Niinemets Ü.: Desiccation–rehydration measurements in bryophytes: current status and future insights. – J. Exp. Bot. **73**: 4338-4361, 2022.

Murchie E.H., Niyogi K.K.: Manipulation of photoprotection to improve plant photosynthesis. – Plant Physiol. **155**: 86-92, 2011.

Nayaka S., Saxena P.: Physiological responses and ecological success of lichen *Stereocaulon foliolosum* and moss *Racomitrium subsecundum* growing in same habitat in Himalaya. – Indian J. Fundam. Appl. Life Sci. **4**: 167-179, 2014.

Niyogi K.K., Grossman A.R., Björkman O.: *Arabidopsis* mutants define a central role for the xanthophyll cycle in the regulation of photosynthetic energy conversion. – Plant Cell **10**: 1121-1134, 1998.

Orekhova A., Hájek J.: Responses of primary photosynthetic processes to repetitive rehydration differ in two representatives of Svalbard moss flora. – Czech Polar Rep. **12**: 103-114, 2022.

Permann C., Pierangelini M., Remias D. *et al.*: Photophysiological investigations of the temperature stress responses of *Zygnema* spp. (Zygnematophyceae) from subpolar and polar habitats (Iceland, Svalbard). – Phycologia **61**: 299-311, 2022.

Proctor M.C.F., Ligrone R., Duckett J.G.: Desiccation tolerance in the moss *Polytrichum formosum*: physiological and fine-structural changes during desiccation and recovery. – Ann. Bot.-London **99**: 75-93, 2007.

Puhovkin A., Bezsmertna O., Parnikoza I.: Interspecific differences in desiccation tolerance of selected Antarctic lichens: analysis of photosystem II effectivity and quenching mechanisms. – Czech Polar Rep. **12**: 31-43, 2022.

Ramakers L.A.I., Harbinson J., Wientjes E., van Amerongen H.: Unravelling the different components of nonphotochemical quenching using a novel analytical pipeline. – New Phytol. **245**: 625-636, 2025.

Ruban A.V.: Quantifying the efficiency of photoprotection. – Philos. T. Roy. Soc. B **372**: 20160393, 2017.

Sahay S., Grzybowski M., Schnable J.C., Głowacka K. : Genotype-specific nonphotochemical quenching responses to nitrogen deficit are linked to chlorophyll *a* to *b* ratios. – J. Plant Physiol. **297**: 154261, 2024.

Seleiman M.F., Al-Suhaibani N., Ali N. *et al.*: Drought stress impacts on plants and different approaches to alleviate its adverse effects. – Plants-Basel **10**: 259, 2021.

Singh G.M., Goldberg S., Schaefer D. *et al.*: Biochemical, gas exchange, and chlorophyll fluorescence analysis of maize genotypes under drought stress reveals important insights into their interaction and homeostasis. – Photosynthetica **60**: 376-388, 2022.

Skotnica J., Matoušková M., Nauš J. *et al.*: Thermoluminescence and fluorescence study of changes in Photosystem II photochemistry in desiccating barley leaves. – Photosynth. Res. **65**: 29-40, 2000.

Swoczyna T., Kalaji H.M., Bussotti F. *et al.*: Environmental stress – what can we learn from chlorophyll *a* fluorescence analysis in woody plants? A review. – Front. Plant Sci. **13**: 1048582, 2022.

Špundová M., Kučerová Z., Nožková V. *et al.*: What to choose for estimating leaf water status-spectral reflectance or *in vivo*

chlorophyll fluorescence? – Plant Phenomics **6**: 0243, 2024.
Takahashi S., Milward S.E., Fan D.-Y. *et al.*: How does cyclic electron flow alleviate photoinhibition in *Arabidopsis*? – Plant Physiol. **149**: 1560-1567, 2009.
Tezara W., Mitchell V.J., Driscoll S.D., Lawlor D.W.: Water stress inhibits plant photosynthesis by decreasing coupling factor and ATP. – Nature **401**: 914-917, 1999.
Townsend A.J., Saccon F., Giovagnetti V. *et al.*: The causes of altered chlorophyll fluorescence quenching induction in the *Arabidopsis* mutant lacking all minor antenna complexes. – BBA-Bioenergetics **1859**: 666-675, 2018.
Trueba S., Pan R., Scoffoni C. *et al.*: Thresholds for leaf damage due to dehydration: declines of hydraulic function, stomatal conductance and cellular integrity precede those for photochemistry. – New Phytol. **223**: 134-149, 2019.
Wang B., Yang X., Chen L. *et al.*: Physiological mechanism of drought-resistant rice coping with drought stress. – J. Plant Growth Regul. **41**: 2638-2651, 2022.
Wang Z., Li G., Sun H. *et al.*: Effects of drought stress on photosynthesis and photosynthetic electron transport chain in young apple tree leaves. – Biol. Open **7**: bio035279, 2018.
Woo N.S., Badger M.R., Pogson B.J.: A rapid, non-invasive procedure for quantitative assessment of drought survival using chlorophyll fluorescence. – Plant Methods **4**: 27, 2008.
Xu Z.Z., Zhou G.S., Wang Y.L. *et al.*: Changes in chlorophyll fluorescence in maize plants with imposed rapid dehydration at different leaf ages. – J. Plant Growth Regul. **27**: 83-92, 2008.
Xue S., Zang Y., Chen J. *et al.*: Effects of enhanced UV-B radiation on photosynthetic performance and non-photochemical quenching process of intertidal red macroalgae *Neoporphyra haitanensis*. – Environ. Exp. Bot. **199**: 104888, 2022.
Yamakawa H., Fukushima Y., Itoh S., Heber U.: Three different mechanisms of energy dissipation of a desiccation-tolerant moss serve one common purpose: to protect reaction centres against photo-oxidation. – J. Exp. Bot. **63**: 3765-3775, 2012.
Yamakawa H., Itoh S.: Dissipation of excess excitation energy by drought-induced nonphotochemical quenching in two species of drought-tolerant moss: desiccation-induced acceleration of photosystem II fluorescence decay. – Biochemistry **52**: 4451-4459, 2013.
Zait Y., Shemer O.E., Cochavi A.: Dynamic responses of chlorophyll fluorescence parameters to drought across diverse plant families. – Physiol. Plantarum **176**: e14527, 2024.
Zaks J., Amarnath K., Sylak-Glassman E.J., Fleming G.R.: Models and measurements of energy-dependent quenching. – Photosynth. Res. **116**: 389-409, 2013.
Zhang L., Yang C., Liu C.: Revealing the significance of chlorophyll *b* in the moss *Physcomitrium patens* by knocking out two functional chlorophyllide *a* oxygenase. – Photosynth. Res. **158**: 171-180, 2023.
Zivcak M., Olsovska K., Brestic M., Slabbert M.M.: Critical temperature derived from the selected chlorophyll *a* fluorescence parameters of indigenous vegetable species of South Africa treated with high temperature. – In: Photosynthesis Research for Food, Fuel and the Future. Advanced Topics in Science and Technology in China. Pp. 628-632. Springer, Berlin-Heidelberg 2010.
Zlatev Z.: Drought-induced changes in chlorophyll fluorescence of young wheat plants. – Biotechnol. Biotec. Eq. **23**: 438-441, 2009.
Zlatev Z., Lidon F.C.: An overview on drought induced changes in plant growth, water relations and photosynthesis. – Emir. J. Food Agric. **24**: 57-72, 2012.